Di-layers satellite electronic shielding system (DiLSES): fabrication and characterization

Emmanuel Ochoyo Adamu [a,*], Abubakar Sadiq Aliyu[a], Abdulkarim Muhammad Hamza[a], Muhammad Sani[a], Umar Sa'ad Aliyu[a], Mngusuur Scholastica Iorshase[a], Lubem James Utume[a], Wasiu Oyeyemi Salami[b], Isaac Pada[c], Emmanuel Ogwuche[d]

[a]*Department of Physics, Faculty of Sciences, Federal University of Lafia, P. M. B 146, Lafia, Nasarawa State, Nigeria*
[b]*Department of Polymer Technology, Nigerian Institute of Leather and Science Technology, Zaria*
[c]*Department of Medical Physics National Hospital, Abuja*
[d]*Department of Science Laboratory and Technology, College of Environmental Sciences and Technology Makurdi, Benue State*

A B S T R A C T

Satellites in space are vulnerable to high-energy electrons above 1 MeV that can damage their electronic systems. To curtail this challenge, a new multi-layer system is synthesized from biomass and geological ores and characterized for mechanical, thermal as well as gamma and beta radiation shielding efficiencies. The new system, a Di-layer Satellite Electronic Shielding System (DiLSES), featuring an innovative, light weight, two-layer material composite made from low atomic number material labeled $L/(DF - H)$ which are arranged in two configurations LH and HL. This advanced material shows exceptional mechanical characteristics with impact strength of 0.6498 J/mm, hardness of 75.4 Hv, and tensile strength of 23.5 MPa, making it resistant to launch vibrations and collision with low velocity space debris. Thermogravimetric analysis (TGA) revels that DiLSES can withstand high temperature environment of up to 300 and only gradually decomposes by less than 5% between 400 and 500. For gamma radiation shielding efficiency, the DiLSES effectively attenuated pointed gamma radiation from Co-60 with maximum energy of 1.332 MeV by 17.71% and 8.74% for $Cs - 137$ (0.6614 Mev), and the LH configuration offers better attenuation. The DiLSES attenuates high-energy beta particles generated by medical LINAC by over 93%, achieving a remarkable 98.24% reduction at 10 Mev energy .This innovative light-weights and cost-effective material has the potential to improve the shielding of electronic components in satellites against high-energy beta particles (greater than 1 Mev) which cause satellite damage and operational failures. It also offers protection from space radiation like gamma and cosmic rays, making it useful for both space and medical applications.

Keywords: Satellites, Space radiation, Linear attenuation, Beta radiation.

1. INTRODUCTION

Satellites play a pivotal role in modern telecommunications, navigation, Earth observation, and scientific research [1]. As satellites operate in the harsh environment of space, they are exposed to various forms of radiation, including solar radiation, cosmic rays, and charged particles. These radiation sources pose significant threats to the sensitive electronics components on board of satellites thereby causing malfunctions or permanent damage.

The use of low atomic number (z) material like lithium as primary component in space radiation shielding has gained substantial attention in recent years [2]. Lithium, a naturally occurring

*Corresponding Author Tel. No.: +234-706-0767-198.
  e-mail:* adamueo9@gmail.com (Emmanuel Ochoyo Adamu)

element, is known for its effectiveness in absorbing and attenuating high-energy beta particles and it has low chances of releasing secondary particles due to low z. This unique property makes it a promising candidate for enhancing the beta radiation shielding applications in areas where the release of secondary particles are controlled. Lithium ore, which typically contains lithium-bearing minerals such as spodumene and lepidolite, offers the advantage of being readily available and cost-effective. Extracting lithium from these ores has become an area of interest for researchers aiming to develop innovative radiation shielding solutions. Additionally, the combination of lithium ore with High-Density Polyethylene (HDPe) reinforced bio-fiber sourced from the leaves of Doum palm fruit has been used to manufacture DiLSES which would be characterized for radiation shielding in satellite communication.

High-Density Polyethylene (HDPe) is a versatile polymer recognized for its exceptional properties and diverse applications in various industries [2]. Its relevance in radiation shielding has gained substantial attention, particularly in contexts involving ionizing radiation attenuation. HDPe possesses inherent attributes that makes it a promising candidate for radiation shielding applications due to its unique combination of high atomic number, hydrogen-rich composition, and density [3].

Despite recent advancements in space radiation shielding, current materials often suffer from weight constraints or limited effectiveness, restricting satellite design and performance. To address this critical issue, this study aimed to bridge the gap by fabricating and characterizing a novel dilayered shielding material, utilizing lithium ore and Doum Fiber reinforced HDPe to enhance satellite reliability in the face of radiation challenges.

2. MATERIALS AND METHOD
The materials used in this was Spodumene, Doum sourced fiber, analytical grade HDPe (99.9% purity) and Epochem 205 epoxy resin.

2.1. PREPARATION OF DOUM FIBER
Doum leaves were specifically selected from Lau Local Government Area, Taraba State, Nigeria, due to their high fiber content and potential for reinforcement in composite materials. Studies have demonstrated that Doum palm fibers possess favorable mechanical properties, making them effective reinforcements in polymeric matrices [4]. Only mature and healthy leaves were chosen, then sorted, washed, sun-dried, and shredded into 5mm pieces using a Laboratory Milling Machine.

The composites samples were mixed in a mixer and HDPe pellets were added while the rolls of the two rolls mill machine were in counter clockwise motion and soften for a period of 5 minutes at a temperature of $210°C$. Upon achieving a band and bank formation of the polymer on the front roll, the prepared doum fiber was introduced gradually to the bank; cross mixed and allowed to mix for 3 minutes. The composite was sheeted out and labeled accordingly. The HDPe composite obtained from the mixing process was placed into a metal mould of dimensions 120mm x100mm x 5mm and was placed on the hydraulic hot press (Compression Molding Machine) for shaping at temperature of 160 and pressure of 2.5 MPa for 5mins. The sample was then transfer to a hydraulic non-hot press (Compression Molding Machine) for cooling by conduction it was cooled, removed from the mould and labeled accordingly.

2.2. LITHIUM ORE AND EPOCHEM 205 EPOXY RESIN COMPOSITION
The lithium layer of DiLSES was prepared using a mixture of 50 g of epoxy resin in the ratio of 2:1 of epoxy and hardener, and thoroughly mixing in a mixing bowl using a mechanical stirrer of 500 rpm. Upon achieving a homogenous mixture, 200g of the Lithium ore was added accordingly and mixed at 210℃ for 3 minutes until a uniform filler distribution is obtained.

2.2.1. Hot pressing
The composite mixture of lithium ore was poured into a mould measuring 120 mm × 100 mm × 5 mm, which was covered with aluminum foil and coated with release oil to facilitate easy removal of the composite after formation. The sample was cast at room temperature and allowed to gel and solidify completely over two (2) hours. Afterward, it was removed from the mould, placed on a flat surface, and left to cure for twenty-four (24) hours at room temperature.

After fabrication, layers of lithium ore and doum fiber reinforced HDPe was bounded using two orientations with the synthesized HDPe using black gum. The DiLSES was then cut into different shapes and sizes for characterization.

2.3. CHARACTERIZATION OF DILSES
The impact test was carried out in accordance with ASTM D-156 using an Izod Impact Tester (Model: XYZ123, SN: 456789). The sample of DiLSES was cut to dimensions 64 mm × 12.7 mm × 3.2 mm and 45°. The hardness test was conducted in accordance with ASTM D2240 using a Micro Vickers Hardness Tester (Model: ABC456, SN: 654321). The tensile strength test was performed in accordance with ASTM D638 using a Universal Testing Machine (Model: D-100KN, SN: 190536) by applying a tensile load until fracture. The tensile strength was calculated as the maximum load divided by the original cross-sectional area. Thermogravimetric Analysis (TGA) was carried out in accordance with ASTM E1131 using a TGA Analyzer (Model: TGA-500, SN: 789101) by heating the sample from room temperature to 800°C at a rate of 10°C/min under a nitrogen atmosphere. The weight change was recorded continuously to determine the thermal stability, decomposition temperature, and composition of the material. Three samples were tested, and the average decomposition temperature was recorded.

The beta radiation shielding efficiency of DiLSES was measured using an Elekta Synergy Platform linear accelerator (Model: Elekta-MLC80, SN: 112233), equipped with an 80-leaf multi-leaf collimator (MLC). The system operated at photon energies of 6 MV, 10 MV, and 15 MV, as well as electron energies of 6 MeV, 9 MeV, 12 MeV, 15 MeV, and 18 MeV, under controlled room temperature conditions. The samples were placed at a fixed distance from the radiation source, and the transmitted intensity was recorded using a radiation detector. Two samples of different thicknesses and face orientations were tested, and the attenuation coefficient was determined by measuring the reduction in radiation intensity through each sample.
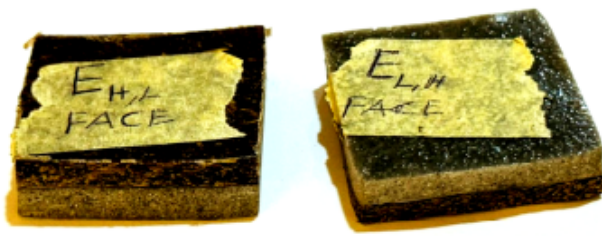
Figure 1. Fabricated di-layers radiations shielding materials (left) HL FACE (right) LH FACE.

Table 1. Physical and mechanical properties testing.

Test Type	Test Parameter	Value
Impact Test	Impact Strength (J/mm)	0.6498
Hardness Test	Hardness (Hv)	75.40
Tensile Test	Tensile Strength	25.89

For gamma radiation shielding, the shielding efficiency was tested using Cs-137 and Co-60 sources. The samples (Figure 1) were placed between the source and a high-purity germanium (HPGe) detector (Model: HPGe-5000, SN: 445566), and the transmitted radiation intensity was measured. Two samples were tested for each of the two sources, and the attenuation coefficient was determined by comparing the initial and transmitted gamma ray intensities.

3. RESULT AND DISCUSSION

3.1. PHYSICAL AND MECHANICAL PROPERTIES

The impact strength of the Di-layer material was reported to be 0.6498 J/mm, indicating a moderate level of toughness necessary for components exposed to mechanical shocks during launch or potential debris impacts. This finding is consistent with the observations of [5], who emphasized the importance of toughness in satellite materials. The hardness test yielded a Vickers hardness (Hv) value of 75.4, suggesting that the material exhibits substantial resistance to surface deformation, ensuring durability in radiation shielding applications, as noted by Ref. [6]. Table 1 summarizes the mechanical properties of DiLSES highlighting the structural integrity of the composite.

Additionally, the tensile strength of the composite material was assessed at 23.5 MPa, reflecting its ability to withstand tensile loads without failure. This result aligns with findings from Ref. [7], who indicated that a balance between flexibility and rigidity is crucial for materials used in environments where slight deformation is acceptable.

3.2. THICKNESS AND DENSITY

The study evaluated two configurations: HL (1.04 cm thickness, 1.101 g/cm^3 density) and LH (0.98 cm thickness, 1.064 g/cm^3 density), as shown in Table 2 [8]. The HL configuration, being slightly thicker and denser, was reported to provide enhanced mechanical strength and potentially better radiation shielding [9]. Conversely, the LH configuration was noted for being lighter

Table 2. Thickness and density.

S/N	Material	Thickness (cm)	Density (g/cm^3)
1	HL	1.04 ± 0.00471	1.101 ± 0111
2	LH	0.98 ± 0.00471	1.064 ± 0.036

without significant compromise on protection. The thickness of a material is determined by

$$t = \frac{V}{A}, \tag{1}$$

where t is thickness (*mm or cm*), V is volume (cm^3 *or* mm^3), A is cross-sectional area (cm^2 *or* mm^2), and the density is given by:

$$\rho = \frac{m}{V}, \tag{2}$$

where m is the mass of the material in grams (g), V is the volume in cubic centimeters (cm^3).

Density plays a significant role in the effectiveness of radiation shielding materials. Higher density materials typically provide better radiation attenuation due to their greater mass per unit volume [10].

3.3. THERMAL ANALYSIS AND DIFFERENTIAL THERMAL ANALYSIS

The dilayered material, with one side made of lithium ore and the other of Doum fiber-reinforced HDPe, showed excellent stability up to 300°C, with no significant weight loss. Ref. [11] reported similar thermal resistance, which is critical for applications in space environments. Decomposition began gradually between 400°C and 500°C, suggesting the breakdown of lower molecular weight components, likely including HDPe and Doum fiber. This behavior is typical for polymer composites [12]. The percentage weight loss is calculated using

$$WeightLoss\,(\%) = \frac{InitialWeight - FinalWeight}{InitialWeight} \times 100. \tag{3}$$

This measurement is crucial for determining how materials behave under thermal stress. Studies indicate that materials with lower weight loss percentages exhibit higher thermal stability [13], which is vital for applications in environments subjected to temperature fluctuations [14].

A sharp weight loss was observed from 600°C to 800°C, indicative of the primary thermal degradation of the polymer matrix and the decomposition of organic components within the material [15]. Mentioned that beyond 800°C the weight stabilized, resulting in a residual mass of approximately 75-80%, attributed to stable inorganic fillers like lithium ore. The DTA analysis backed this up, showing key thermal events during these stages. These findings confirm that the composite material exhibits thermal stability, retaining shielding capabilities under elevated temperatures, which is essential for space applications, as illustrated in Figure 2 [6].

3.4. ELECTRON ATTENUATION SHIELDING

The evaluation of LH and HL materials' shielding capabilities against electron beam radiation the analysis focuses on key parameters, including Linear Attenuation Coefficient (LAC), Mass
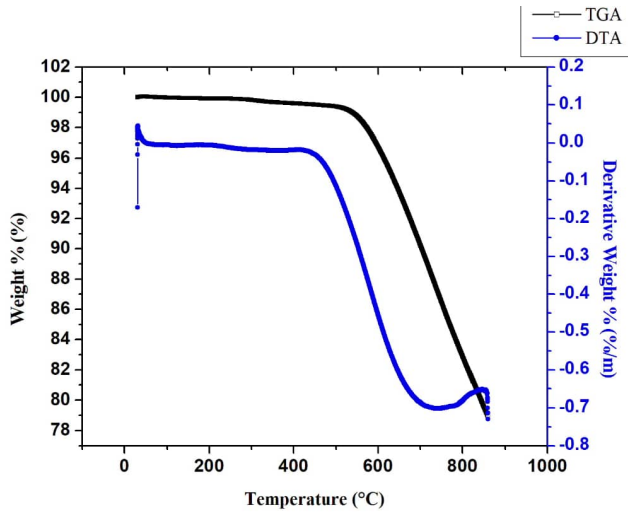
Figure 2. TGA and DTA curve.

Figure 3. Plot of LAC verse energy level (MeV) for fabricated materials.

Attenuation Coefficient (μ/ρ), Half-value Layer (HVL), Tenth-value Layer (TVL), Mean Free Path (MFP), and Radiation Protection Efficiency (RPE). As shown in Table 3, the findings, supported by similar observations in recent literatures [16, 17], highlight the materials' effectiveness and reliability for shielding applications.

3.4.1. Linear attenuation coefficient (LAC)

It is reported that HL configuration exhibited higher attenuation coefficients across all energy levels, confirming its superior attenuation capability. For example, at 6 MeV, HL achieved an LAC of 3.395 cm^{-1}, which was higher than LH's LAC of 3.199 cm^{-1}. At 15 MeV, the LAC values decreased, but HL still maintained a better performance with 2.778 cm^{-1} compared to LH 2.615 cm^{-1} as illustrated in Figure 3. Ref. [18] also reported that materials with high densities and atomic numbers exhibit enhanced attenuation properties, aligning with the observed results. These findings suggest that HL is particularly effective in attenuating high-energy electrons. It was calculated using the equation:

$$LAC = \frac{\ln(D_o/D)}{x}, \qquad (4)$$

where D_o denotes the initial radiation dose, D is transmitted dose after passing through the material, x = Thickness of the material. The LAC can vary based on radiation type, energy level, and material properties. Materials with higher attenuation coefficients provide better radiation shielding.

3.4.2. Mass attenuation coefficient (μ/ρ)

The mass attenuation coefficient results showed that HL consistently recorded higher values than LH. For instance, at 6 MeV, HL achieved μ/ρ = 3.1911 cm^2/g, while LH exhibited μ/ρ = 2.906 cm^2/g, as shown in Figure 4.

These values affirm the materials efficiency in absorbing electron energy relative to their mass [19], supports the observation that materials with higher μ/ρ values are ideal for shielding applications as they ensure efficient energy absorption. This result
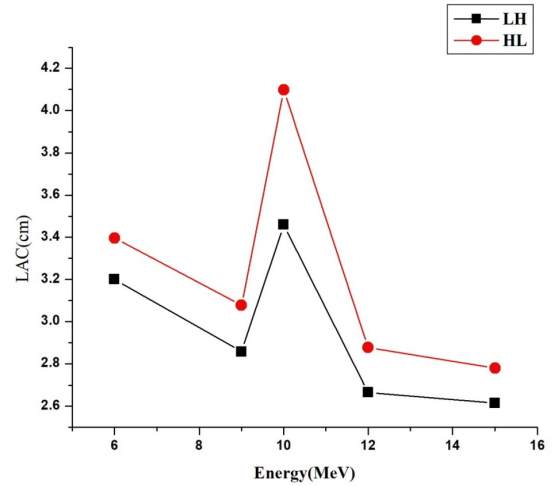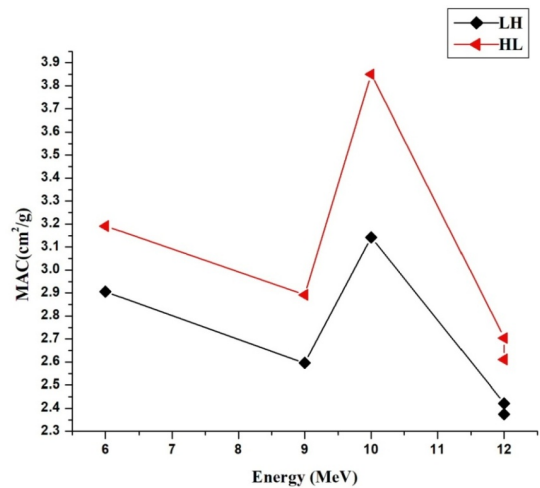

Figure 4. Plot of MAC verse energy level (MeV) for fabricated materials.

underlines the advantage of HL for environments requiring effective electron radiation shielding with the formula:

$$MAC = \frac{\mu}{\rho}, \qquad (5)$$

where μ is linear attenuation coefficient (cm^{-1}), ρ is material density (g/cm^3).

This parameter accounts for both the material's attenuation ability and its density. Higher MAC values indicate better shielding efficiency.

3.4.3. Half-value layer (HVL)

It was observed that both LH and HL materials have low HVL values, which indicates their efficiency in reducing electron intensity. HL, with an HVL of 0.204 cm at 6 MeV, and 0.17 cm at 10 MeV required slightly less thickness than LH, which recorded an HVL of 0.216 cm at 6 MeV and 0.20 cm at 10 MeV (Figure 5). According to [18], materials with lower HVLs are more efficient for shielding because they reduce the required thickness while

Table 3. Electron attenuation shielding.

| Energy	Sample ID	LAC (cm⁻¹)	MAC (cm/g)	HVL (cm)	TVL (cm)	MFP (cm)	RPE(%)
6	LH	3.199600553	2.906085879	0.216635536	0.719647673	0.312539013	96.41203349
	HL	3.395494464	3.191254196	0.204137332	0.678129538	0.294507916	96.08696985
9	LH	2.857466055	2.595337017	0.242574073	0.805813629	0.349960413	94.87871447
	HL	3.077596013	2.892477455	0.225223576	0.748176526	0.324928937	95.10053462
10	LH	3.459740736	3.142362158	0.200346567	0.665536891	0.289038999	97.26251444
	HL	4.096989717	3.850554245	0.169184506	0.562018763	0.244081648	98.19579462
12	LH	2.665980182	2.421417059	0.259997124	0.863691752	0.375096562	93.75019166
	HL	2.876513925	2.703490531	0.240967782	0.800477645	0.347643024	94.03334458
15	LH	2.615135413	2.375236524	0.265052118	0.880484078	0.382389377	93.41081705
	HL	2.778575492	2.611443131	0.249461345	0.828692652	0.359896646	93.43228352
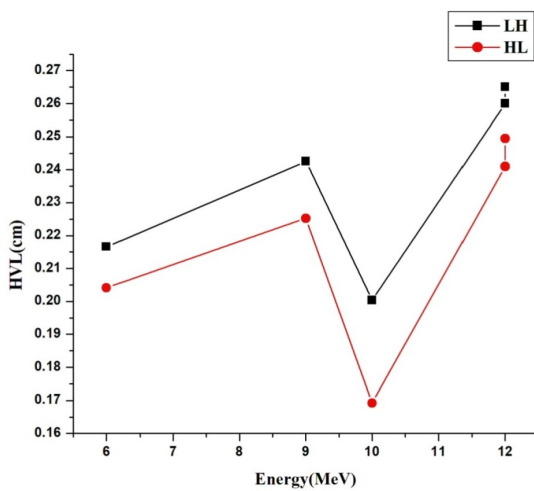
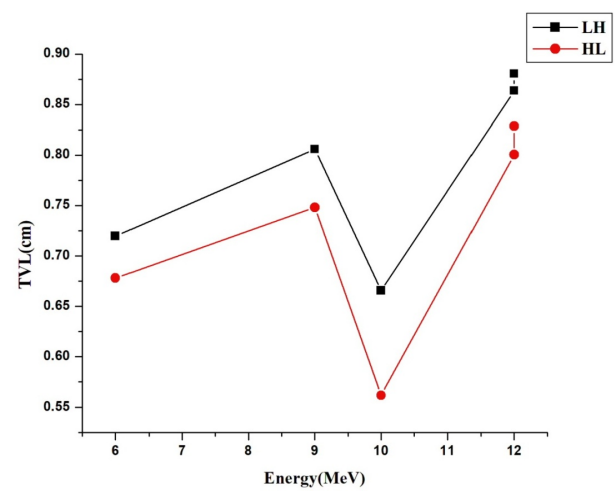**Figure 5. Half- value layer (HVL) for the fabricated di-layered materials.**

Figure 6. Tenth- value layer (TVL) of the fabricated di-layered materials.

maintaining protection levels. This behavior underscores HL's suitability for applications where minimizing material usage is critical. It is given by the formula:

$$HVL = \frac{\ln(2)}{\mu},\qquad(6)$$

where μ is linear attenuation coefficient (cm⁻¹). Smaller HVL values indicate better shielding properties, as less material is needed to achieve significant attenuation.

3.4.4. Tenth-value layer (TVL)

The analysis of TVL revealed that both materials are highly effective in reducing electron beam intensity. At 6 MeV, HL exhibited a TVL of 0.678 cm, slightly lower than LH which has TVL of 0.719 cm. This trend was consistent at higher energy levels, confirming the reliability of both materials as shown in Figure 6. Similar observations have been reported by Ref. [17], who noted that materials with low TVL values are preferred for achieving optimal radiation attenuation. This behavior highlights the potential of HL for high-energy shielding applications. It was calculated using:

$$TVL = \frac{\ln(10)}{\mu},\qquad(7)$$

where μ is linear attenuation coefficient (cm^{-1}).

Lower TVL values indicate more efficient shielding. As with HVL, materials that require thinner layers for substantial attenuation are preferable.

3.4.5. Mean free path (MFP)

The mean free path results demonstrated that HL consistently exhibited shorter MFP values, indicating a higher interaction rate with electrons. For instance, at 6 MeV, HL recorded an MFP of 0.294 cm, compared to LH 0.312 cm as illustrated in Figure 7. Ref. [7] corroborate that shorter MFP values are characteristic of materials with superior shielding capabilities. This behavior further supports the use of HL in environments requiring frequent electron attenuation. The formula is:

$$MFP = \frac{1}{\mu}.\qquad(8)$$

A smaller MFP indicates that the material causes more frequent interactions, which leads to better radiation attenuation [18].

3.4.6. Radiation protection efficiency (RPE)

Both materials achieved remarkably high RPE values across all energy levels, exceeding 93% in every case. At 6 MeV, HL recorded an RPE of 96.08%, closely aligning with LH
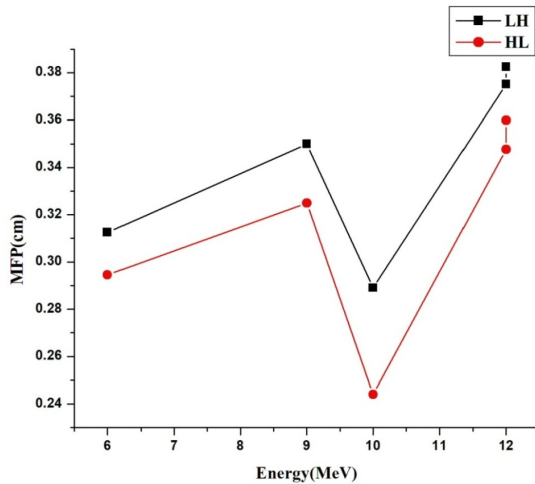
Figure 7. Mean free path (MFP) of the fabricated di-layered materials.
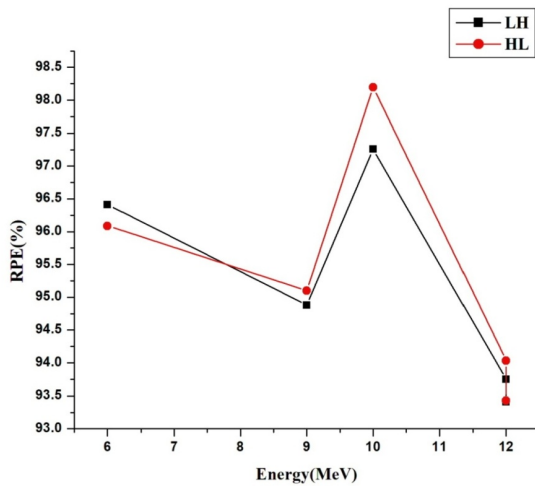

Figure 8. Radiation protection efficiency (RPE) of the fabricated di-layered materials.

96.41%. These results confirm the materials' strong performance in shielding applications as shown in Figure 8. Ref.[16] have similarly reported that materials with RPE values above 90% are considered highly efficient for radiation protection This observation further validates the exceptional shielding capabilities of LH and HL materials. It is obtained using the equation:

$$RPE = \left(1 - \frac{D}{D_o}\right) \times 100, \tag{9}$$

where D_0 is initial dose, D is transmitted dose after passing through the material. Higher RPE values indicate more effective radiation shielding, as a larger percentage of the radiation is blocked [16].

3.5. GAMMA ATTENUATION EFFICIENCY

The shielding effectiveness of two materials, HL and LH, under gamma radiation from Cs-137 and Co-60 sources shielding performance was evaluated using key parameters, Linear Atten-

uation Coefficient (LAC), Mass Attenuation Coefficient (MAC), Half-Value Layer (HVL), Tenth-Value Layer (TVL), Mean Free Path (MFP), and Radiation Protection Efficiency (RPE). The results, shown in Table 4, highlight the superior performance of HL and its potential for practical applications [20], have emphasized the importance of high-density shielding materials. For instance, documented how high-density composites effectively attenuate gamma rays. This research builds on those findings, validating the applicability of HL as an efficient gamma shielding material.

3.5.1. Linear attenuation coefficient (LAC)

The LAC values reveal that HL consistently outperformed LH. For Co-60, HL achieved an LAC of 0.1874 cm^{-1}, compared to 0.0707 cm^{-1} for LH.

3.5.2. Mass attenuation coefficient (MAC)

The MAC values confirm the superior performance of HL, with values exceeding those of LH across both gamma sources. For Co-60, HL recorded a MAC of 0.1702 cm²/g, while LH showed only 0.0664 cm²/g [19], also reported that materials with high atomic numbers and mass densities typically have better MAC performance, supporting the results observed here.

3.5.3. Half-value layer (HVL)

The HVL values for HL were significantly lower, indicating better shielding performance. For Co-60, HL achieved an HVL of 3.69cm, compared to 9.81cm for LH. Lower HVL values highlight the material's efficiency in reducing gamma-ray intensity with minimal thickness This observation is consistent with the finding of [21], who stressed the importance of lower HVL values in designing compact and efficient radiation shields.

3.5.4. Tenth-value layer (TVL)

The TVL results reinforced the superior attenuation capabilities of HL. For Co-60, HL required a TVL of 12.28 cm, compared to 32.58 cm for LH. The reduced thickness required for radiation attenuation makes HL an excellent choice for applications where space and weight constraints are critical [3].

3.5.5. Mean free path (MFP)

The values also demonstrated the enhanced photon interaction capability of HL, with HL recording shorter MFPs across both gamma sources. For Co-60, HL had an MFP of 5.33 cm, compared to 14.15cm for LH. Such short MFPs are indicative of better gamma-ray attenuation [20].

3.5.6. Radiation protection efficiency (RPE)

Finally, the RPE values confirm the superior performance of HL. For Co-60, HL achieved an RPE of 17.71%, which was significantly higher than the 6.69% observed for LH. In Fig:13 High RPE values, as emphasized by Ref. [10], are critical for ensuring effective radiation protection, making HL a credible choice for shielding applications.

4. CONCLUSION

This research focused on developing and characterizing a Di-layer Satellite Electronic Shielding System (DiLSES), using a

Table 4. Gamma attenuation shielding.

Energy	Sample ID	LAC (cm^{-1})	MAC (cm/g)	HVL (cm)	TVL (cm)	MFP (cm)	RPE(%)
CS-137	HL	0.082331931	0.077379634	8.418935060	27.96709690	12.14595586	7.751604151
	LH	0.086601716	0.078657326	8.003850451	26.58821568	11.54711535	8.612893502
Co-60	HL	0.070667718	0.066417028	9.808540622	32.58326666	14.15073291	6.691069390
	LH	0.187442976	0.170247935	3.697909592	12.28418977	5.334955831	17.71165427

composite material of lithium ore and Doum fiber-reinforced HDPE, designed for radiation shielding in space. The results indicated that DiLSES offers promising mechanical and radiation protection properties, making it a strong candidate for satellite shielding. Both HL and LH configurations showed desirable mechanical strength, TGA confirmed the material's ability to retain its integrity at higher temperatures, aligning with the characteristics of polymer composites. For electron and gamma radiation shielding efficiency, the DiLSES showed high effectiveness, with the HL configuration outperforming LH in key attenuation properties, particularly for high-energy radiation. Both configurations exhibited excellent structural durability, beyond space technology, the material has potential applications in aerospace engineering, nuclear facilities, and medical radiation shielding for diagnostic imaging rooms, radiotherapy equipment by reducing radiation-induced malfunctions.

DATA AVAILABILITY

Data will be made available by the corresponding author on request.

References

[1] S. Dymkova, "Earth observation and global navigation satellite systems analitical report part I (aviation & space)", Synchroinfo J. **8** (2022) 30. http://dx.doi.org/10.36724/2664-066X-2022-8-1-30-41.

[2] C. Schuy, C. Tessa, F. Horst, M. Rovituso, M. Durante, M. Giraudo, L. Bocchini, M. Baricco, A. Castellero, G. Fioreh & U. Weber, "Experimental assessment of lithium hydride's space radiation shielding performance and monte carlo benchmarking", Radiat. Res. **191** (2018) 154. https://doi.org/10.1667/RR15123.1.

[3] A. M. El-Khatib, M. M. Gouda, M. S. Fouad, M. Abd-Elzaher & W. Ramadan, "Radiation attenuation properties of chemically prepared MgO nanoparticles/HDPE composites", Sci. Rep. **13** (2023) 9945. 10.1038/s41598-023-37088-y. https://doi.org/10.1038/s41598-023-37088-y.

[4] H. Elmoudnia, Y. Millogo, P. Faria, R. Jalal, M. Waqif & L. Saâdi, "Development of doum palm fiber-based building insulation composites with citric acid/glycerol eco-friendly binder", J. Compos. Sci. **9** (2025) 67. https://doi.org/10.3390/jcs9020067.

[5] Esha & J. Hausmann, "Material characterization required for designing satellites from fiber-reinforced polymers", J. Compos. Sci. **7** (2023) 515. https://doi.org/10.3390/jcs7120515.

[6] G. Barra, L. Guadagno, M. Raimondo, M. G. Santonicola, E. Toto, & S. Vecchio Ciprioti, "A comprehensive review on the thermal stability assessment of polymers and composites for aeronautics and space applications", Polymers (Basel). **15** (2023) 3786. https://doi.org/10.3390/polym15183786.

[7] F. Chen, J. Fan, D. Hui, C. Wang, F. Yuan & X. Wu, "Mechanisms of the improved stiffness of flexible polymers under impact loading", Nanotechnol. Rev. **11** (2022) 3281. https://doi.org/10.1515/ntrev-2022-0437.

[8] M. I. Sayyed, "The impact of chemical composition, density and thickness on the radiation shielding properties of CaO–Al2O3–SiO2 glasses", Silicon **15** (2023) 7917. https://doi.org/10.1007/s12633-023-02640-y.

[9] S. C. Kim & H. Byun, "Development of ultra-thin radiation-shielding paper through nanofiber modeling of morpho butterfly wing structure", Sci. Rep. **12** (2022) 22532. https://doi.org/10.1038/s41598-022-27174-y.

[10] N. Ahmad, M. I. Idris, A. Hussin, J. Abdul Karim, N. M. Azreen & R. Zainon, "Enhancing shielding efficiency of ordinary and barite concrete in radiation shielding utilizations", Sci. Rep. **14** (2024) 26029. https://doi.org/10.1038/s41598-024-76402-0.

[11] Y. Park, J. H. Kim, H. S. Lee, E. Y. Jung, H. Lee, D. O. Noh, & H. J. Suh, "Thermal stability of yeast hydrolysate as a novel anti-obesity material", Food Chem. **136** (2013) 316. https://doi.org/10.1016/j.foodchem.2012.08.047.

[12] E. A. M. Farrag, "Ionizing radiation shielding properties of CdZnSe chalcogenide glass", Radiat. Eff. Defects Solids **2025** (2025) 1. https://doi.org/10.1080/10420150.2024.2448118.

[13] J. Tan & Y. Zhang, "Thermal conductive polymer composites: recent progress and applications", Molecules **29** (2024) 3572. https://doi.org/10.3390/molecules29153572.

[14] N. V. Siharova, P. Pączkowski, Y. I. Sementsov, S. V. Zhuravsky, M. V. Borysenko, A. D. Terets, O. V. Mischanchuk, M. I. Terets, Y. V. Hrebelna & B. Gawdzik, "Thermal degradation of polymer composites based on unsaturated-polyester-resin- and vinyl-ester-resin- filled kraft lignin", Materials **18** (2025) 524. https://doi.org/10.3390/ma18030524.

[15] R. Ogabi, B. Manescau, K. Chetehouna & N. Gascoin, "A study of thermal degradation and fire behaviour of polymer composites and their gaseous emission assessment", Energies **14** (2021) 7070. https://doi.org/10.3390/en14217070.

[16] L. Sidauruk, H. A. Sianturi, M. Rianna, T. Sembiring & D. A. Barus, "Determination of half value layer (hvl) value on X-rays radiography with using aluminum, copper and lead (Al, Cu, and Sn) attenuators", J. Phys. Conf. Ser. **1116** (2018) 032032. https://iopscience.iop.org/article/10.1088/1742-6596/1116/3/032032.

[17] A. M. Abd El-Hameed, "Radiation effects on composite materials used in space systems: a review", NRIAG J. Astron. Geophys. **11** (2022) 313. https://doi.org/10.1080/20909977.2022.2079902.

[18] P. S. Dahinde, G. P. Dapke, S. D. Raut, R. R. Bhosale & P. P. Pawar, "Analysis of half value layer (hvl), tenth value layer (tvl) and mean free path (mfp) of some oxides in the energy range of 122keV to 1330keV", Indian J. Sci. Res. **9** (2019) 79. http://dx.doi.org/10.32606/IJSR.V9.I2.00014.

[19] P. Pöml & X. Llovet, "Determination of mass attenuation coefficients of Th, U, Np, and Pu for Oxygen K α X-Rays using an electron microprobe", Microsc. Microanal. **26** (2020) 194. https://doi.org/10.1017/S1431927620001282.

[20] I. G. Alhindawy, M. I. Sayyed, A. H. Almuqrin & K. A. Mahmoud, "Optimizing gamma radiation shielding with cobalt-titania hybrid nanomaterials", Sci. Rep. **13** (2023) 8936. https://doi.org/10.1038/s41598-023-33864-y.

[21] S. Sen, J. S. O'Dell, Y. Yan, L. Heilbronn, H. Ning, M. Finckenor, M. Carrico & S. Pillay, "Space environmental effects on multifunctional radiation shielding materials", Earth Sp. Sci. **11** (2024) e2024EA003681. https://doi.org/10.1029/2024EA003681.